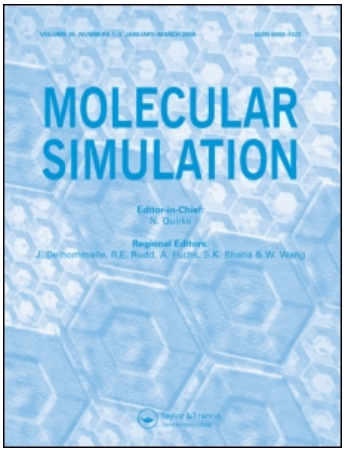

Molecular Simulation
Publication details, including instructions for authors and subscription information:
http://www.informaworld.com/smpp/title~content=t713644482

Synthesis and Characterization of Templated Mesoporous Materials Using Molecular Simulation

Flor R. Siperstein[a]; Keith E. Gubbins[a]
[a] Department of Chemical Engineering, North Carolina State University, Raleigh, NC, USA

To cite this Article Siperstein, Flor R. and Gubbins, Keith E.(2001) 'Synthesis and Characterization of Templated Mesoporous Materials Using Molecular Simulation', Molecular Simulation, 27: 5, 339 — 352
To link to this Article: DOI: 10.1080/08927020108031357
URL: http://dx.doi.org/10.1080/08927020108031357

Molecular Simulation, Vol. 27, pp. 339–352
Reprints available directly from the publisher
Photocopying permitted by license only

SYNTHESIS AND CHARACTERIZATION OF TEMPLATED MESOPOROUS MATERIALS USING MOLECULAR SIMULATION

FLOR R. SIPERSTEIN and KEITH E. GUBBINS*

Department of Chemical Engineering, North Carolina State University, Raleigh, NC 27695-7905, USA

(Received June 2001; In final form July 2001)

Lattice Monte Carlo simulations are used to calculate equilibrium properties of surfactant–solvent–silica liquid–crystal systems under no-polymerization conditions. The formation of a high-surfactant high-silica concentration phase in equilibrium with a dilute phase is observed when the surfactant–silica interactions are stronger than the surfactant–solvent interactions. Different silica structures that are similar to the M41 family are observed, depending on the overall concentration of the system. The formation of a hexagonal phase is favored at a surfactant/silica ratio of 0.2, whereas a lamellar phase is observed a surfactant/silica ratio of 1.

Argon adsorption properties on a model porous structure of the MCM-41 type prepared using this mimetic simulation protocol are calculated using grand canonical Monte Carlo simulation. Heats of adsorption are calculated from fluctuations in the energy and number of molecules [1] following the work of Nicholson and Parsonage [*Computer Simulation and the Statistical Mechanics of Adsorption* (Academic Press, London), 1982, p 97 8 pp]. A decrease in the heats of adsorption for coverage less than one statistical monolayer is evidence of surface heterogeneity. The results are in qualitative agreement with experimental measurements for argon on MCM-41.

Keywords: Templated materials; Surfactant; Silica; Hexagonal phase

INTRODUCTION

Templated mesoporous materials have attracted a lot of attention from the scientific community since their introduction in 1992 by researchers at Mobil [2] although synthesis of similar materials has been reported earlier in the literature dating back to a patent filed in 1969 [3] which was later shown to yield a material

*Corresponding author.

with the same properties as MCM-41 [4] and the synthesis of FSM-16 in 1990 [5]. Several synthesis procedures have been proposed since then, using a variety of surfactant-inorganic pairs. Although some syntheses have been performed using a *true liquid crystal templating* technique [6] where the initial surfactant solution is at a high enough concentration to form liquid crystal phases, most syntheses start with a dilute surfactant solution [7]. In this case, the final structure of the porous solid does not resemble the micellar structure in the surfactant solution used for the synthesis. The prediction of the final structure of the porous materials is complicated because the physics underlying these syntheses is not well understood, mainly due to the overlapping self-assembly and inorganic polymerization processes.

The key to predicting structures of templated mesoporous materials is to understand how a dilute solution with spherical micelles becomes a liquid crystal phase when silica is added to the system. The detailed simulation of micelle formation alone is a challenging problem for today's computer power. Simulations using detailed atomistic potentials have, for the most part, focused on the evolution of prearranged structures, but are usually unable to span real times that are long enough to observe formation and destruction of micelles [8]. Coarse-grained approaches, either on- or off-lattice, are normally used to study the formation of micelles. Although off-lattice simulations are typically more versatile and realistic, lattice simulations allow larger systems to be studied, and can be made more realistic through lattice discretization [9].

Lattice Monte Carlo simulations have been used to study micellization processes and to determine binary and ternary phase diagrams containing spherical micelles, hexagonal, lamellar and cubic structures. Generally the model surfactant molecules are made up of m hydrophilic head groups H and n hydrophobic tail groups T, i.e. H_mT_n, and are distributed across lattice sites with one group per site. Solvent molecules, S, occupy single sites, and oil molecules if present occupy one or several sites [10–17]. Recently lattice Monte Carlo simulations have been used to study evaporation driven self-assembly to describe dip-coating synthesis of templated materials [18].

In this work, we show that synthesis of templated materials in bulk solution can be interpreted with an equilibrium triangular diagram for surfactant, solvent and silica where different liquid crystal phases can be located. The liquid crystal-like behavior of silica-surfactant phases has been observed experimentally under no polymerization conditions [19]. The equilibrium diagram is calculated using a lattice Monte Carlo approach, specifying the appropriate interaction parameters to represent each component. Two extreme cases are studied, one where the three binaries are completely miscible and another where the solvent and the inorganic oxide (silica) are immiscible. In the former case, a favorable interaction between

the silica and the surfactant head produces an immiscibility gap inside the ternary diagram, while in the latter case a larger region of phase separation occurs due to the immiscibility between the solvent and the oxide. The shape and location of the immiscibility gap determines the different liquid crystal phases that can be formed.

Model porous materials are obtained by assuming that the silica polymerization is sufficiently fast that no modification of the liquid crystal structure occurs. Silica polymerization is followed by removal of the surfactant chains. Adsorption isotherms and heats of adsorption of argon on a model material with cylindrical pores are calculated using grand canonical Monte Carlo simulations. Heats of adsorption, calculated from fluctuations in the energy and number of molecules [1] during the GCMC simulations, decrease with coverage for loadings below one statistical monolayer, in agreement with experimentally measured heats of adsorption of argon and krypton on MCM-41 [20,21].

SIMULATION TECHNIQUE

Lattice Monte Carlo

We used Larson's lattice model [10] with a fully occupied cubic lattice in which a site interacts equally with all 26 sites that lie within one lattice spacing in directions (1,0,0), (1,1,0) and (1,1,1). Each segment of the surfactant (H_mT_n), solvent (S) or silica (inorganic oxide, I) occupies a single point on the lattice. H_4T_4 was used as a model surfactant molecule, which consists of a sequence of four hydrophilic head segments H, and four hydrophobic tail segments T. A site on the surfactant chain can be connected to any of its $z = 26$ nearest-neighbors or diagonally nearest-neighbors.

Each molecular unit (H, T, S and I) is characterized by an interaction energy ε_{ab} (a, b = H, T, S, I). The net energy change associated with any configuration rearrangement depends on a set of interchange energies ω_{ab} :

$$\omega_{ab} = \varepsilon_{ab} - \frac{1}{2}(\varepsilon_{aa} + \varepsilon_{bb}) \quad \text{with a} \neq \text{b} \tag{1}$$

and not on the individual interaction energies ε_{ab}. The surfactant–solvent interaction parameters are the same as those used by other researchers [14–16]: $\omega_{HT}/k_BT = \omega_{ST}/k_BT = 0.153846$ and $\omega_{HS} = 0$. A strong inorganic-head attraction to mimic the strong affinity between silica and surfactant heads was specified as $\omega_{IH}/k_BT = -0.307692$ and $\omega_{IT} = 0.153846$. Two extreme cases were studied, one where the inorganic component and the solvent are completely

miscible ($\omega_{IS} = 0$) and another where they are immiscible ($\omega_{IS}/k_BT = 0.153846$). The reduced temperature is defined using the head−tail DA6" \char"32}tailinterchangeenergyby$T^* = k_BT/\omega_{HT}$.

All Monte Carlo simulations were performed in the canonical ensemble (NVT) with periodic boundary conditions. Reputation and "kink" -like moves were considered in addition to chain regrowth using the configurational bias method [22]. Ternary liquid–liquid equilibria were calculated using a direct interfacial approach. One dimension of the simulation box was increased with respect to the other two by a factor of eight to make the formation of planar interfaces preferable to curved interfaces [15]. The box size used in the simulation was $40 \times 40 \times 320$. Bulk coexisting densities were estimated from ensemble averages of the system densities away from the interfaces. The reduced temperature was chosen to be the same as that used by Larson in his work ($T^* = 6.5$). Up to 125,000 cycles were needed for the system to equilibrate, where each cycle consists of $40 \times 40 \times 320$ configurations.

Different density profiles were used as the initial configuration for the ternary liquid–liquid equilibrium calculations, as a check that the system had reached equilibrium. The starting configuration was obtained as follows. A high surfactant concentration slab was obtained by equilibrating at infinite temperature a $40 \times 40 \times 40$ or $40 \times 40 \times 80$ box with periodic boundary conditions in the x and y directions and hard walls in the z direction. Typically, the high-surfactant concentration box contained 60% in volume of surfactant while the rest was solvent. After equilibration, the box with the high surfactant concentration was placed in the $40 \times 40 \times 320$ box, resulting in a slab having 60% surfactant. Silica and solvent units were distributed randomly over the whole $40 \times 40 \times 320$ box not allowing for overlaps with the previously arranged surfactant chains. This selection of initial configuration favored the formation of only two interfaces (Fig. 1). The final surfactant concentration in the high surfactant concentration slab varied between 40 and 80% in volume when phase separation was observed. Formation of spherical micelles was observed in the absence of silica.

Some simulations were carried out starting from a completely homogeneous box, but the equilibration time was considerably larger and the formation of more than two interfaces was observed. Nevertheless, the compositions far from the interface were the same for different initial configurations.

The materials obtained from the direct interfacial simulation do not present perfectly flat interfaces, and are not convenient to use for adsorption measurements because the interface curvature generates unrealistic large pores when periodic boundary conditions are used in the x, y and z directions. Removing the interface curvature does not yield a proper periodic material.

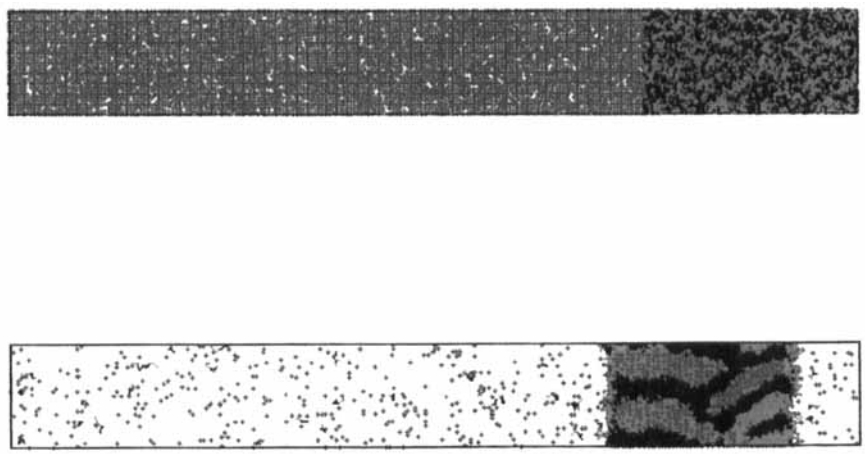

FIGURE 1 Initial configuration (top) and snapshot after 15×10^9 configurations (bottom) at $T^* = 6.5$ for the system with complete miscibility between solvent and silica. Surfactant heads are in yellow, surfactant tails are in red and silica units are in gray. The system is converging into a lamellar phase.

Therefore, some simulations were carried out at the bulk density of the high-surfactant high-silica phase obtained from the liquid–liquid equilibrium calculation to obtain model materials without having the problems due to the interfaces. These simulations were performed in a cubic box (between 20^3 and 80^3) with periodic boundary conditions. A typical run consisted of $2–7 \times 10^8$ configurations for the system to equilibrate.

After the system reached equilibrium it was assumed that connected silica units polymerize without modification of the mesostructure, and the surfactant and unconnected silica units were removed from the system.

Material Characterization

Adsorption isotherms and heats of adsorption of argon in a prototype material with cylindrical pores obtained from the mimetic synthesis were calculated using grand canonical Monte Carlo simulations. The material was obtained at a surfactant concentration of 55% and silica concentration of 35%, with the remainder being solvent. The structure of the material as obtained from the lattice simulation is shown in Fig. 2. The material shows cylindrical pores with diameter of eight lattice segments.

The positions of the silica segments obtained from the lattice simulation were scaled to obtain a material with a pore diameter of 4 nm. Thus, the distance between each lattice point was assumed to be 0.5 nm. A sphere of 0.5 nm is

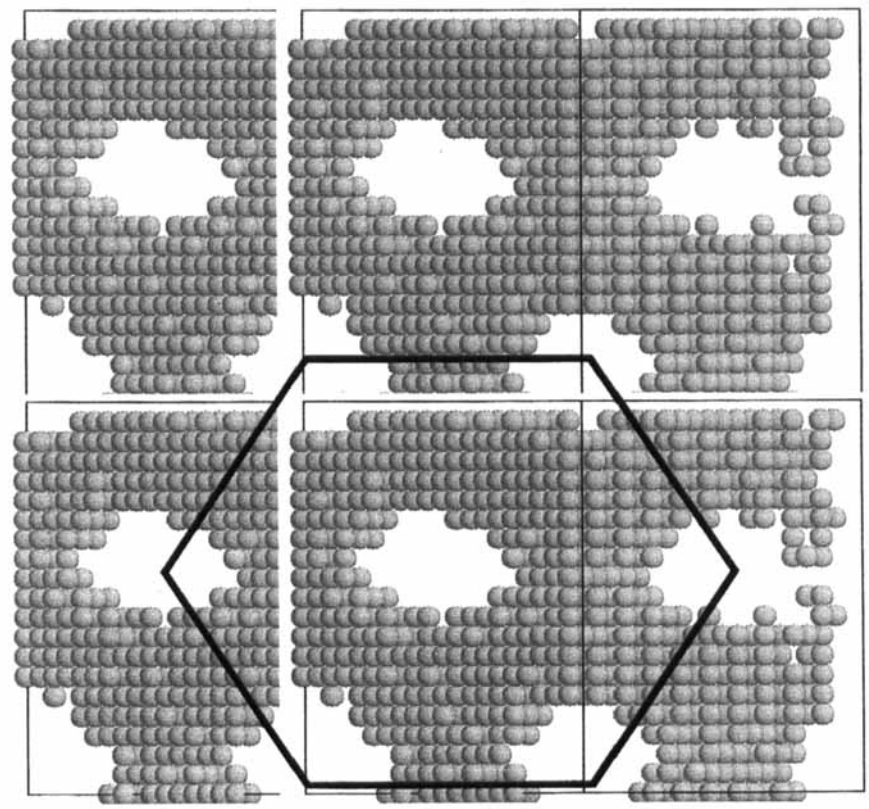

FIGURE 2 Model silica structure showing the hexagonal arrangement of independent cylindrical pores. $2 \times 2 \times 1$ simulation boxes are shown.

considerably larger than the oxygen diameter in silica materials (0.27 nm); therefore, it was assumed that each silica sphere corresponded to a collection of silica units. The distance between connected silica spheres in the lattice can be between 1 and 1.73 ($\sqrt{3}$) times the separation between lattice points. Therefore, each silica sphere was assumed to have a hard core center of 0.72 nm to avoid the formation of micropores between each silica sphere. Each sphere has a density of 2.7 g/cm^3 [23] and the interactions between these spheres and adsorbed fluids were modeled following the work of Kaminsky and Monson [24], where the solid–fluid potential is given by:

$$u_{sf}(r) = \frac{16}{3}\pi\epsilon_{sf}\rho_s R^3 \left(\frac{(r^6 + (21/5)r^4R^2 + 3r^2R^4 + (1/3)R^6)\sigma_{sf}^{12}}{(r^2 - R^2)^9} - \frac{\sigma_{sf}^6}{(r^2 - R^2)^3} \right) \tag{2}$$

where R is the hard core radius of the solid sphere and ρ_s, its density; ε_{sf} and σ_{sf} are the Lennard–Jones interaction parameters between a fluid molecule and an oxygen atom in a siliceous material that were taken from argon–oxygen interaction parameters in silicalite [25]. Parameters used for the simulation are summarized in Table I. The solid sphere radius, R, was taken as 3.25 Å to allow some overlap between the silica spheres.

Simulations were performed using periodic boundary conditions. The system was allowed to equilibrate during the first 1×10^5–1×10^6 cycles of each simulation point. Statistics were taken over the following one million cycles. Each cycle corresponded to a displacement and a creation or deletion. Each simulation was divided into ten blocks. Partial averages in each block were used to calculate standard deviations in total amount adsorbed and energy of the system. Simulations were carried out at 77 K for pressures up to 0.5 bar.

Heats of adsorption were calculated as [1]:

$$q_{st} = -\frac{f(N,U)}{f(N,N) - \bar{N}^G} + kT \tag{3}$$

where the fluctuations are defined as $f(X,Y) = \langle XY \rangle - \langle X \rangle \langle Y \rangle$ and $\bar{N}^G$ is the number of molecules at the bulk gas density in the same volume as the system. In our case, $\bar{N}^G$ was ignored because it is negligible compared with $f(N,N)$.

RESULTS

Synthesis of Silica Materials

The phase diagram obtained for solvent-H_4T_4 was in good agreement with the one reported by Larson [14]. Addition of a silica source to a surfactant solution results in a phase separation where a surfactant-rich silica-rich phase is in equilibrium with a surfactant-poor silica-poor phase [19]. The surfactant rich phase presents liquid crystal type behavior.

Phase separation in a ternary system where two binaries are completely miscible can be achieved either by an effective attraction between two components strong enough to form a two-phase region, or by an effective

TABLE I Constants of Lennard–Jones 12–6 potential [25]

	σ (nm)	ε/k (K)
Fluid–fluid	0.3405	119.8
Fluid–solid	0.3335	93.0

repulsion between molecules of two different components that is sufficiently strong to induce the phase separation. The former process is known as associative and the latter as segregative phase separation [26]. These types of phase separation have been observed in systems containing a polyelectrolyte (hyaluronate) and a cationic surfactant (alkyltrimethyammonium-bromide) [27].

Ternary diagrams for associative and segregative phase separations are shown in Fig. 3. The formation of a surfactant-rich phase is observed in both cases. This phase can adopt different liquid–crystal type structures, such as lamellar, perforated lamella, and hexagonal The formation of a bicontinuous phase was observed, but not of a cubic phase. The formation of a cubic phase is not observed when the size of the simulation box does not correspond to an integer multiple of the unit cell parameters of the cubic structure. More detailed studies are needed in the borders between lamellar and hexagonal phases to observe the formation of cubic phases.

The associative phase diagram is similar to the behavior observed for the ternary system water–sodium hyaluronate (NaHy)–alkyltrimethylammonium bromide (CTAB) in the absence of salt [27]. This behavior was expected, since at the synthesis conditions the silica source is a highly charged oligomer. An important difference between the solvent–silica–CTAB and water–NaHy–CTAB systems is that for the latter the high-surfactant concentration phase contains no more than 30% of surfactant, which probably is not enough to observe the formation of surfactant liquid–crystal phases.

Some general trends observed experimentally were found in our mimetic synthesis. For example, variation of the surfactant/silica ratio result in the formation of different mesophases [28]. Hexagonal phases are observed for low surfactant/silica ratios (*ca.* 0.6) and lamellar phases are observed for higher surfactant/silica ratios (*ca.* 1.3). We observe a lamellar phase for surfactant/silica ratios of 1.0 and hexagonal phases for surfactant/silica ratios of 0.13–0.20. These ratios are practically independent of whether the mixture is associative or segregative. The exact boundaries for these phases have not been calculated. At high surfactant/silica ratios (*ca.* 2) perforated lamella are observed and for surfactant/silica ratios of 10 it is observed that the silica is deposited between adjacent micelles.

No cubic phases were found, which experimentally are observed at a surfactant/silica ratio of 1.0. The cubic octamer, observed experimentally at a surfactant/silica ratio of 1.9, is not observed, mainly due to the lack of structure of the silica in our simulations and to the different number of possible interactions between one surfactant chain and silica units. Experimental evidence shows that one silica unit interacts with the ammonium group of one surfactant chain, while in our simulations the limit is specified by the connectivity of the lattice. Another

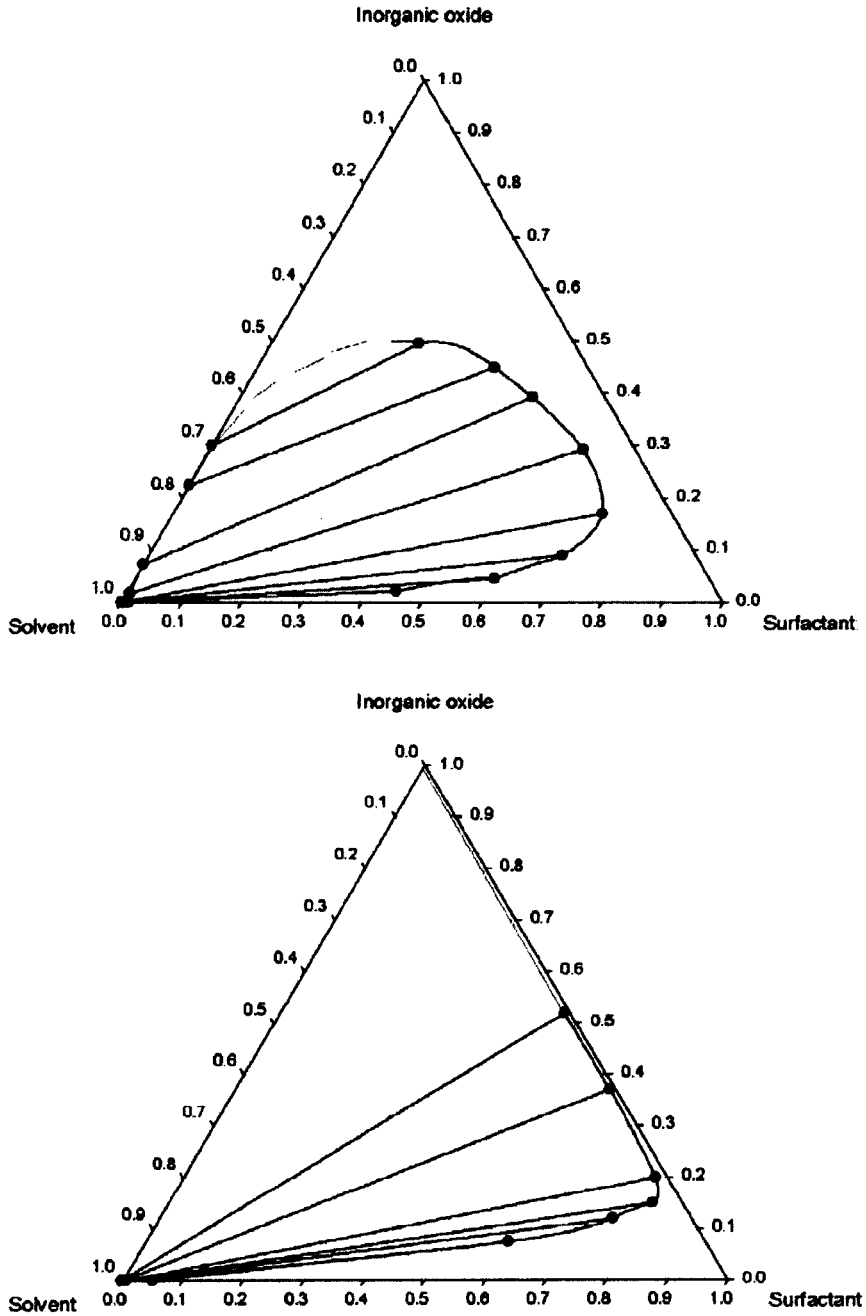

FIGURE 3 Associative (top) and segregative (bottom) phase diagrams for H_4T_4–solvent–silica at $T^* = 6.5$.

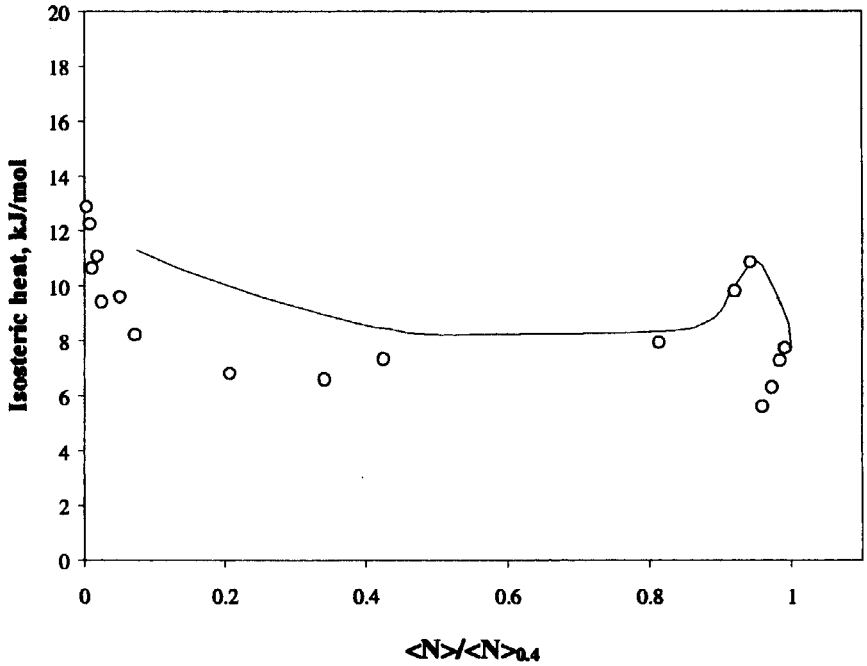

FIGURE 4 Isosteric heats of adsorption for argon on MCM-41 type material at 77 K. Symbols are simulation results and solid line shows experimental results [20]. The simulated amount adsorbed is normalized by the amount adsorbed at $f/f^0 = 0.4$ and experimental results at $P/P^0 = 0.8$.

important difference is that a commonly used source of silica for the synthesis of templated materials is TEOS (tetraethoxiorthosilane), which produces ethanol upon polymerization. The addition of an alcohol to a surfactant system changes the solubility of the surfactant and the structure of the micelles and liquid crystal phases, which is a phenomena not accounted for in our simulations.

Material Characterization

Simulation studies of gas adsorption on MCM-41 type materials using an idealized pore geometry show that surface energetic heterogeneity needs to be considered in order to describe correctly low coverage nitrogen adsorption isotherms [23]. Heats of adsorption of simple fluids (argon [20] and krypton [21]) on MCM-41 decrease by approximately 3 kJ/mol on going from zero coverage to half saturation, confirming the adsorbent heterogeneity.

Heats of adsorption on homogeneous cylinders calculated using non-local DFT [29] increase with coverage as a result of adsorbate–adsorbate interactions.

When surface heterogeneity is present, as in corrugated surfaces, heats of adsorption decrease with coverage [30].

Heats of adsorption calculated in our model material decrease with coverage from about 13 down to 6 kJ/mol (Fig. 4). Our model presents less high-energy sites than what would be expected from experimental measurements, consequently, the decrease in the heats of adsorption in our modeled material extends only to approximately 20% of saturation whereas in real materials it extends to 40% of saturation.

An argon adsorption isotherm calculated on our model material is compared with experimental isotherms in Fig. 5. The calculated isotherm has qualitatively the same shape as the experimental one, and differences between experimental and simulated isotherms are consistent with the differences observed in the heats of adsorption. The uptake at low pressures is less than what is observed experimentally, which is consistent with a smaller number of high-energy sites compared with real materials.

Snapshots of the simulation at low and high relative pressure are shown in Fig. 6. The influence of the lattice used for the synthesis is evident from the solid

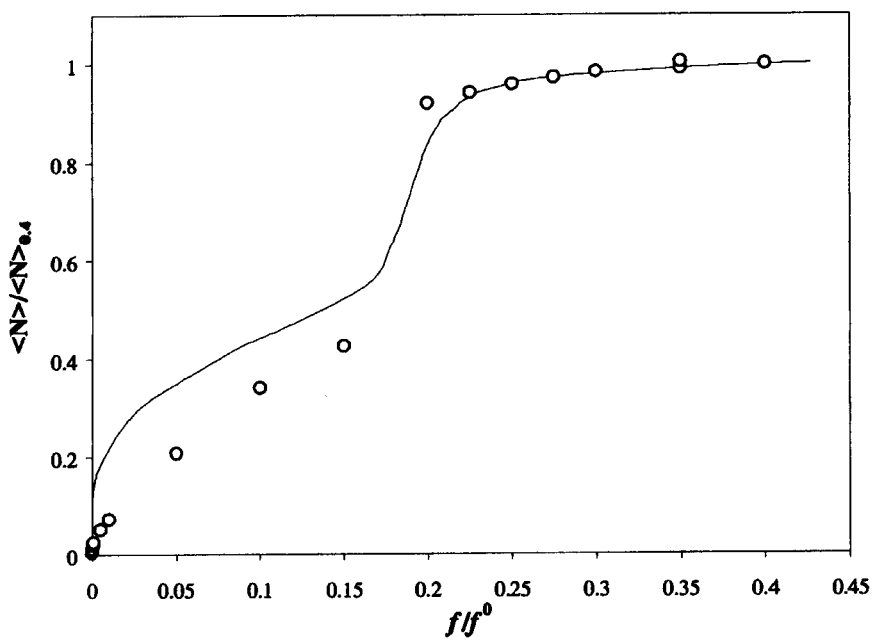

FIGURE 5 Argon adsorption isotherms at 77 K for argon on MCM-41. Open symbols are simulation results and the solid line is an experimental isotherm taken from Ref. [20].

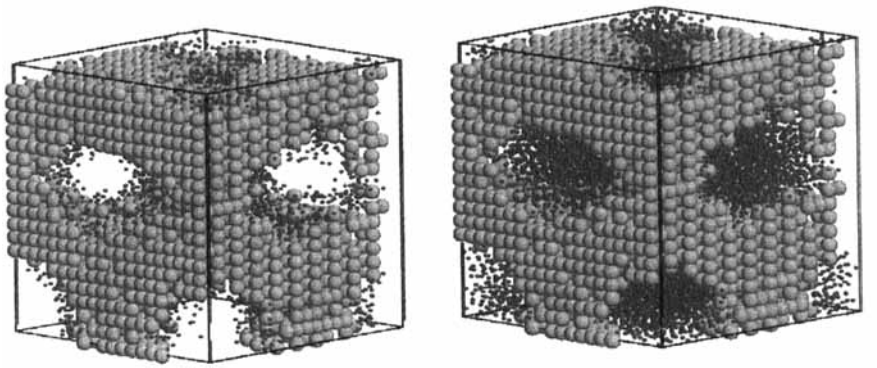

FIGURE 6 Snapshot of adsorption simulation at $f/f^0 = 0.1$ (left) and $f/f^0 = 0.2$ (right). Solid silica structure is in gray and argon is in blue. Argon atoms are shown to a reduced scale for better visualization.

structure. At low relative pressures a cylindrical monolayer is formed and at high relative pressures the complete pore is filled with argon.

CONCLUSIONS

We have developed a methodology to determine silica porous structures following a typical templating material synthesis in bulk solution. The range of structures obtained is in qualitative agreement with experimental observations: hexagonal phases are observed at low surfactant/silica ratios and lamellar phases at high surfactant/silica ratios.

Grand canonical Monte Carlo simulations of argon adsorption were used to characterize the materials obtained with the mimetic simulation. Adsorption properties in the materials modeled are comparable with experimental measurements and they indicate that the adsorbent has less high-energy sites than real materials. A more detailed description of the silica spheres may account for a broader surface heterogeneity.

The choice of surfactant produces a material with walls that are considerably thicker than in MCM-41 type materials. The wall thickness depends on the length of the hydrophilic section of the surfactant; thus using a surfactant with a smaller head to tail ratio will yield a more realistic material.

The structure of silica materials is not well reproduced by cubic lattices because the tetrahedral arrangement between silica units cannot be reproduced. Future work will be concentrated on using a more realistic description of the silica for the synthesis of templated materials.

Acknowledgements

We thank the Department of Energy for support of this research under grant no. DE-FG02 98ER14847. FRS thanks Martin Lísal for many useful discussions.

References

[1] Nicholson, D. and Parsonage, N.G. (1982) Computer Simulation and the Statistical Mechanics of Adsorption (Academic Press, London), p 97.
[2] Beck, J.S., Vartuli, J.C., Roth, W.J., Leonowicz, M.E., Kresge, C.T., Schmitt, K.D., Chu, C.T.-W., Olson, D.H., Sheppard, E.W., McCullen, S.B., Higgins, J.B. and Schlenker, J.L. (1992) "A new family of mesoporous molecular sieves prepared with liquid crystal templates", *J. Am. Chem. Soc.* **114**, 10834.
[3] Chiola, V., Ritsko, J.E. and Vanderpool, C.D. (1971) US Patent 3 556 725.
[4] DiRenzo, F., Cambon, F.H. and Dutartre, R. (1997) "A 28-year-old synthesis of micelle-templated mesoporous silica", *Micropor. Mater.* **10**, 283.
[5] Yanagisawa, T., Shimizu, T., Kuroda, K. and Kato, C. (1990) "The preparation of alkyltrimethylammonium–kanemite complexes and their conversion to microporous materials", *B. Chem. Soc. Jpn.* **63**, 988.
[6] Attard, G.S., Glyde, J.C. and Goltner, C.G. (1995) "Liquid–crystalline phases as templates for the synthesis of mesoporous silica", *Nature* **378**, 366.
[7] Ciesla, U. and Schüth, F. (1999) "Ordered mesoporous materials", *Micropor. Mesopor. Mater.* **27**, 131.
[8] Shelley, J.C. and Shelley, M.Y. (2000) "Computer simulation of surfactant solutions", *Curr. Opin. Colloid Interf. Sci.* **5**, 101.
[9] Panagiotopoulos, A.Z. (2000) "On the equivalence of continuum and lattice models for fluids", *J. Chem. Phys.* **112**, 7132.
[10] Larson, R.G., Scriven, L.E. and Davis, H.T. (1985) "Monte Carlo simulation of model amphiphile–oil–water systems", *J. Chem. Phys.* **83**, 2411.
[11] Larson, R.G. (1992) "Monte Carlo simulation of microstructural transitions in surfactant systems", *J. Chem. Phys.* **96**, 7904.
[12] Larson, R.G. (1989) "Self assembly of surfactant liquid crystalline phases by Monte Carlo simulation", *J. Chem. Phys.* **91**, 2479.
[13] Talsania, S.K., Wang, Y., Rajagopalan, R. and Mohanty, K.K. (1997) "Monte Carlo simulations for micellar encapsulation", *J. Colloid Interf. Sci.* **190**, 92.
[14] Larson, R.G. (1996) "Monte Carlo simulations of the phase behavior of surfactant solutions", *J. Phys. II France* **6**, 1441.
[15] Mackie, A.D., Onur, K. and Panagiotopoulos, A.Z. (1996) "Phase equilibria of a lattice model for an oil–water–amphiphile mixture", *J. Chem. Phys.* **104**, 3718.
[16] Mackie, A.D., Panagiotopoulos, A.Z. and Szleifer, I. (1997) "Aggregation behavior of a lattice model for amphiphiles", *Langmuir* **13**, 5022.
[17] Floriano, M.A., Onur, K. and Panagiotopoulos, A.Z. (1999) "Micellization in model surfactant systems", *Langmuir* **15**, 3143.
[18] Malanoski, A.P. and Van Swol, F. (2000) "Lattice models for adsorption and transport in self-assembled nano-structures", *AIChE Annual Meeting*.
[19] Firouzi, A., Atef, F., Oertii, A.G., Stucky, G.D. and Chmelka, B.F. (1997) "Alkaline lyotropic silicate–surfactant liquid crystals", *J. Am. Chem. Soc.* **119**, 3596.
[20] Neimark, A.V., Ravikovitch, P.I., Grün, M., Schüth, F. and Unger, K.K. (1998) "Pore Size analysis of MCM-41 type adsorbents by means of nitrogen and argon adsorption", *J. Colloid Interf. Sci.* **207**, 159.
[21] Olivier, J.P. (2000) "Thermodynamic properties of confined fluids. I. Experimental measurements of krypton adsorbed by mesoporous silica from 80 K to 130 K", in: *Proceedings of the Second Pacific Basin Conference on Adsorption Science and Technology* Do, D.D., ed, (World Scientific, Singapore), pp 472–476.

[22] Frenkel, D. and Smit, B. (1996) Understanding Molecular Simulation (Academic Press, San Diego).
[23] Maddox, M.W., Olivier, J.P. and Gubbins, K.E. (1997) "Characterization of MCM-41 using molecular simulation: heterogeneity effects", *Langmuir* **13**, 1737.
[24] Kaminsky, R.D. and Monson, P.A. (1991) "The influence of adsorbent microstructure upon adsorption equilibria: investigations of a model system", *J. Chem. Phys.* **95**, 2936.
[25] Talu, O. and Myers, A.L. (1998) "Force constants for adsorption of helium and argon in high-silica zeolites", Fundamentals of Adsorption 6, Meunier, F., ed, (Elsevier, Paris) pp 861–866.
[26] Picullel, L. and Lindman, B. (1992) "Association and segregation in aqueous polymer/polymer, polymer/surfactant and surfactant/surfactant mixtures: similarities and differences", *Adv. Colloid Interf. Sci.* **41**, 149.
[27] Thalberg, K., Lindman, B. and Karlstrom, G. (1990) "Phase diagram of a system of cationic surfactant and anionic polyelectrolyte—tetradecyltrimethylammonium bromide–hyaluronan–water", *J. Phys. Chem.* **94**, 4289.
[28] Vartuli, J.C., Schmitt, K.D., Kresge, C.T., Roth, W.J., Leonowicz, M.E., McCullen, S.B., Hellring, S.D., Beck, J.S., Schlenker, J.L., Olson, D.H. and Sheppard, E.W. (1994) "Effect of surfactant/silica molar ratios on the formation of mesoporous molecular sieves: inorganic mimicry of surfactant liquid–crystal phases and mechanistic implications", *Chem. Mater.* **6**, 2317.
[29] Balbuena, P.B. and Gubbins, K.E. (1994) "The effect of pore geometry on adsorption behavior", Characterization of Porous Solids III, Studies in Surface Science and Catalysis, Rouguerol, J., Rodriguez-Reinoso, F., Sing, K.S.W. and Unger, K. POK., eds, (Elsevier, Amsterdam) **87**, pp 41–50.
[30] Steele, W. and Bojan, M.J. (1997) "Computer simulation study of sorption in cylindrical pores with varying pore wall heterogeneity", Characterization of Porous Solids IV (The Roy Chemical Society, Cambridge), pp 49–56.